

UNIVERSITY OF CALIFORNIA SAN DIEGO

Continuous Skin Eversion Enables an Untethered Soft Robot to Burrow in Granular Media

A Thesis submitted in partial satisfaction of the
requirements for the degree Master of Science

in

Engineering Sciences (Mechanical Engineering)

by

Korkut Eken

Committee in charge:

Professor Michael T. Tolley, Chair
Professor Nicholas Gravish, Co-Chair
Professor Tania K. Morimoto

2023

Copyright

Korkut Eken, 2023

All rights reserved.

The Thesis of Korkut Eken is approved, and it is acceptable in quality and form for publication on microfilm and electronically.

University of California San Diego

2023

DEDICATION

This study is wholeheartedly dedicated to my beloved parents, who have been my source of inspiration and gave me strength when I thought of giving up, who continually provide their moral, emotional, and financial support as well as to my brother, relatives, mentors, friends, and classmates who shared their words of advice and encouragement to finish this study.

EPIGRAPH

Science is the only true guide in life.

Mustafa Kemal Atatürk

TABLE OF CONTENTS

Thesis Approval Page	iii
Dedication	iv
Epigraph	v
Table of Contents	vi
List of Figures	vii
Acknowledgements	viii
Vita	ix
Abstract of the Thesis	x
Introduction	1
Chapter 1 Design and Fabrication	3
Chapter 2 Experimental Results	8
2.1 Comparison of Rigid and Soft Rollers	8
2.2 Effect of Internal Pressure on Locomotion	9
2.3 Performance of the Robot in Digging	11
2.4 Performance of the Robot in Upward Burrowing	14
2.5 Locomotion on Water	16
Conclusion	18
References	19

LIST OF FIGURES

Figure 1.1.	Comparison of robot designs for (a) tethered eversion by tip extension and (b) untethered eversion for locomotion on granular media.	4
Figure 1.2.	(a) Everting prevents relative motion between the skin of the robot and the surrounding granular media resulting in reduced drag. (b) Experimental setup to measure the difference in drag forces between everting and non-everting cases.	5
Figure 1.3.	(a) CAD rendering of the assembled everting mechanism. (b) Exploded isometric view of the everting mechanism. (c) Photo of the fully assembled robot.	6
Figure 2.1.	(a) Process for the fabrication of soft rollers used in the robot to avoid jamming due to sand grains. (b) Experimental setup using Mark-10 force sensor to compare soft and rigid rollers. (c) Plot of experimental results highlighting the difference in force for soft and rigid rollers.	10
Figure 2.2.	(a) Photos of the robot locomoting on sand from above at discrete time points (b) Plot of indentation experiment to determine the relative pressure inside the membrane for three different pressures (c) Plot of distance of the robot vs. time for three trials with different pressures.	12
Figure 2.3.	(a) Photos of the experiment at different discrete time intervals showing the robot’s vertical displacement (b) Plot of vertical displacement vs time for multiple trials with raw and best fit lines shown.	13
Figure 2.4.	Photos of the third trial at different discrete time intervals showing robot burrowing upward over time. Timestamps represents the time after the robot was turned on.	15
Figure 2.5.	Plot of absolute vertical displacement versus time for multiple trials with best fit lines shown dashed lines.	15
Figure 2.6.	Experimental setup showing the difference between the two cases of inflated and deflated robot when comparing the peak pull-out force using the Mark-10 Force sensor.	16
Figure 2.7.	Photos of the experiment at different discrete time intervals showing the robot’s locomotion on water	17

ACKNOWLEDGEMENTS

I would like to acknowledge Professor Michael T. Tolley for his support as the chair of my committee. Through multiple drafts and many meetings, his guidance has proved to be invaluable.

I would like to acknowledge Professor Nicholas Gravish for his support as the co-chair of my committee. It is his support that helped me in an immeasurable way.

I would also like to acknowledge the members of Bioinspired Robotics and Design Lab for their help and support for my research.

I would like to acknowledge Professor Michael T. Tolley and Professor Nicholas Gravish for coauthoring this thesis in full, a major portion of which has been published in the proceedings of the IEEE International Conference on Soft Robotics and on IEEE Xplore. The thesis author was the primary investigator and author of this material.

VITA

- 2021 Bachelor of Science, University of Illinois at Urbana-Champaign
2023 Master of Science, University of California San Diego

PUBLICATIONS

Eken K., Gravish, N., Tolley M. T. (2023) “Continuous Skin Eversion Enables an Untethered Soft Robot to Burrow in Granular Media”, in 2023 IEEE-RAS International Conference on Soft Robotics (RoboSoft).

FIELDS OF STUDY

Major Field: Engineering Sciences (Mechanical Engineering)

Studies in Mechanical Engineering
Professor Michael T. Tolley

ABSTRACT OF THE THESIS

Continuous Skin Eversion Enables an Untethered Soft Robot to Burrow in Granular Media

by

Korkut Eken

Master of Science in Engineering Sciences (Mechanical Engineering)

University of California San Diego, 2023

Professor Michael T. Tolley, Chair
Professor Nicholas Gravish, Co-Chair

Exploration in environments that are too hazardous or inaccessible to humans is one of the most promising uses of robotics. In particular, natural environments that contain granular media are common, but present a variety of challenges for the design and control of robots. Recently, everting vine robots that can navigate many different environments, including digging in sand. However, everting vine robots have previously relied on a tether to provide power and control which limits their ability to explore. Here we present an untethered, continuously everting soft robot for exploration in granular media. We test the ability of this design to reduce the drag on the robot while moving through granular media. We then investigate design features

to improve the ability of the robot to generate thrust in a sand simulant, and validate them experimentally.

Introduction

Robots are useful for exploring in extreme environments such as ocean depths and outer space where the presence of a human is not safe. Engineers have solved many challenges in these environments from exploring Mars using rovers [1] and drones to discovering new species in deep ocean with remotely operated vehicles [2]. However, robotic exploration in granular media is a relatively new research area and it is a challenging problem due to high drag forces [3]. To overcome this challenge, engineers have designed a variety of systems. Most conventional methods such as hydraulic rotary drilling and tunnel boring [4] include heavy machines, making them unsuitable for exploration in small spaces. This work proposes to address the challenge of exploring granular media with an untethered toroidal soft robot.

In previous work, we developed a pneumatically actuated soft robot inspired by the worm that was capable of generating peristaltic motion for digging [5]. However, the robot had limited exploration capabilities because of its relatively low speed as well as its tether. Inspired by nature, other work has created pneumatically actuated worm-like robots, plant root inspired robots that burrow themselves [6, 7], and razor clam inspired soft robot that burrows upward in granular media [8]. In addition, we have previously shown everting (i.e., turning inside-out) robots to be useful for minimally invasive exploration of coral reefs [9]. Other work has shown an everting mechanism to be particularly useful for digging in granular media due to its ability to reduce subterranean drag forces due to the lack of relative motion between the outer skin of the everter and its environment [10]. However, tip-extension eversion is by its nature a tethered approach that relies on a constant supply of pressure from the base to explore. This approach can be limiting as the robot can only explore a certain distance before running out of material to

evert. A retraction mechanism is also required to retract the tip back to the base before relocating the base to a different location [9].

A similar method to navigate confined spaces is simultaneous eversion and inversion (i.e., turning outside-in). This method enables robot to explore freely without the need of retracting back to the original position. Previously, researchers have explored this simultaneous eversion mechanism in many different ways. Orekhov et al. analyzed different actuation mechanisms such as chemically induced actuation, for their “whole skin locomotion” robot [11]. Similarly, Ingram et al. explored actuation of simultaneous eversion mechanism by shape memory alloys (SMAs), pre-tensioned elastic skin, and rings capable of extension and contraction [12]. In addition, Leon-Rodriguez et al. showed the use of ferrofluids to navigate these robots in a magnetic field for medical applications [13]. However, these designs are not suitable to overcome the high forces associated with digging in granular media. More recently, researchers designed a motorized device to navigate a toroidal shaped robot for locomotion in confined spaces [14]. Nonetheless, researchers haven’t explored the locomotion performance of this type of robot in granular media.

This work presents an untethered soft everting robot for exploration in granular media. Our design provides improved performance in granular media. We investigate and experimentally validate design features to improve the ability to locomote in granular media. Lastly, we test our robot’s performance in locomotion and digging. We discuss the design and fabrication of the robot in Chapter 1, experimental results and discussion in Chapter 2-5. In Conclusion, we summarize our findings and provide conclusion.

Chapter 1

Design and Fabrication

When designing a soft robot to be used in granular media, we need to consider many different design choices. Our goal was to design an untethered robot. Previous work on exploration in granular media using everting vine robots [10] use tethered eversion. This limits the distance these robots can explore in granular media before needing to retract to their base. To benefit from force reduction in granular media using eversion and also be free of the constraints of a tether, we chose our design to continuously evert itself in a toroidal shape (Fig. 1.1).

To validate that continuous eversion provided a reduction in drag force when moving through granular media, we conducted a simple experiment (Fig. 1.2) where we pulled a soft toroidal shaped toy (Shop Zoombie 4" Pearlized Water Wiggler) filled with water out of a bed of 0.3 mm glass beads, and measured the drag force using a mechanical testing apparatus (Mark-10 Force Gauge Model M7-50, accuracy of $\pm 0.025\text{N}$, Mark-10 Motorized Test Stand Model ESM750S). We used 0.3 mm glass beads because the particle size of 0.3 mm corresponds with the size of medium sand (0.2 mm to 0.63 mm) according to ISO 14688-1:2017 [15]. The toy was buried at a depth of 10 cm at the deepest point of the toy. This depth was equal to the toy's length. To demonstrate that eversion reduced the drag force, a rod was attached to the bottom of the toy from the inside of the toroidal shape. Therefore, as the mechanical tester pulled the rod out of the granular media at a rate of 200 mm/s, the toy everted (i.e., the outside of the membrane of the toy was stationary with respect to the grains surrounding it, Fig. 1.2(a)).

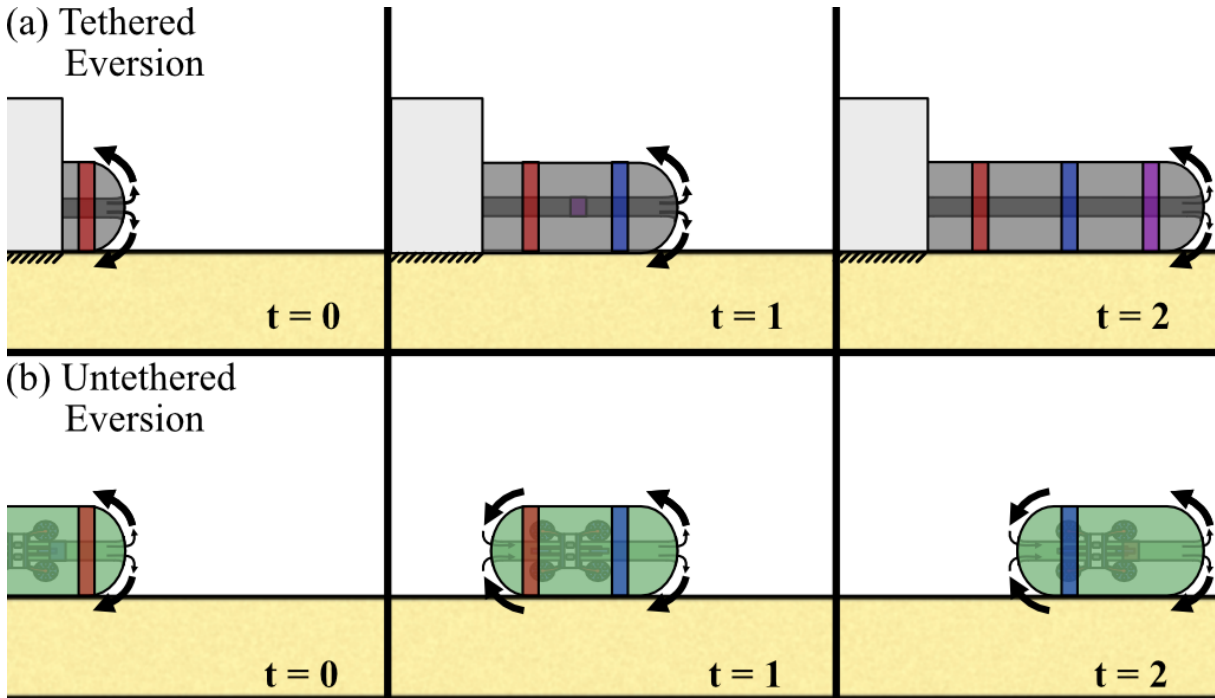


Figure 1.1. Comparison of robot designs for (a) tethered eversion by tip extension and (b) untethered eversion for locomotion on granular media.

To measure the baseline drag without eversion, the toy was attached to the force sensor at the top, which prevented it from everting (i.e., forcing relative motion between the grains and the membrane of the toy). The experiment was repeated three times for each case. We found that eversion provided a reduction in force. It took 1 N on average to pull out to everting toy whereas it took 2.25 N on average to pull out the toy without everting. Based on this result, we chose this toroidal shape for our digging robot.

As for the actuation mechanism of the robot, our design (Fig. 1.3) was inspired by previous work on an untethered toroidal robot [14], a vine robot retraction mechanism [16], and a tip mount for a vine robot [17]. Similar to previous work, our robot used two rollers, each driven by a DC motor, to pull the membrane from its rear, and relied on internal pressure to maintain its shape. As a result, pulling the rear membrane caused the membrane at the front of the robot to evert, and pushed the robot forward. The main body of the robot consists of 6 passive rollers and 2 driven rollers. All of the parts are 3D printed using polylactic acid (PLA)

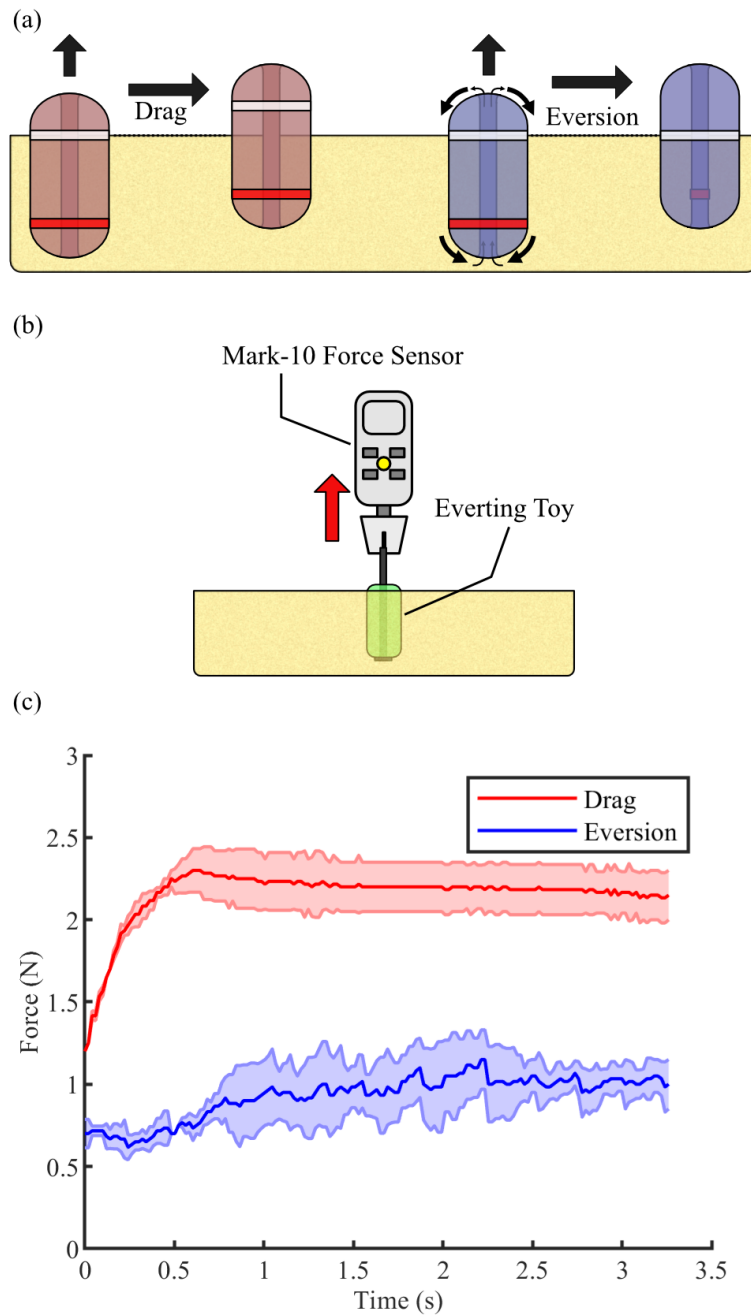


Figure 1.2. (a) Everting prevents relative motion between the skin of the robot and the surrounding granular media resulting in reduced drag. (b) Experimental setup to measure the difference in drag forces between everting and non-everting cases. (c) Results of the experiment showing that the force required to overcome drag in the everting case was reduced as compared to the non-everting case. The solid lines represent the average of four trials whereas the shaded area represents one standard deviation above and below the average.

and the DC motors are powered by three 3.7 V lithium-polymer batteries. The inflated robot had a length of 32 cm and a diameter of 16 cm.

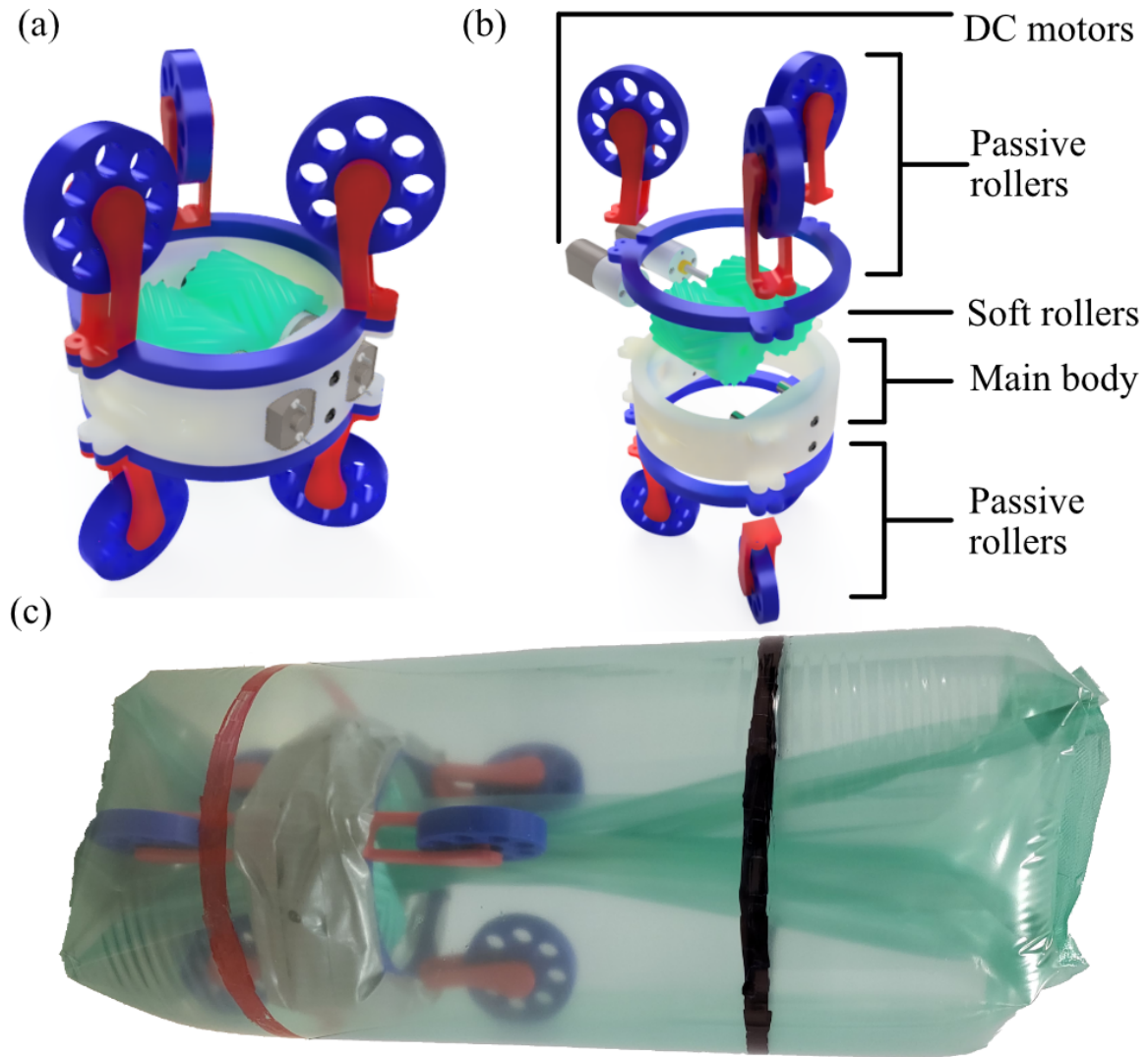


Figure 1.3. (a) CAD rendering of the assembled everting mechanism. (b) Exploded isometric view of the everting mechanism. (c) Photo of the fully assembled robot.

To overcome the challenges of everting in granular media, we investigated adaptations to this basic everting robot design explored in previous work. A major challenge we have faced in our initial prototypes was that grains jammed the main rollers during eversion. The grains entered through the openings at the ends of the toroidal shape and couldn't pass through the rollers, jamming the rollers and stalling the DC motors. As it was not practical to prevent any sand

grains from entering the mechanism, we sought to adapt the feeding mechanism to accommodate some grains. Ultimately we found that this problem could be solved with a soft layer on the rollers of the feeding mechanism. The details of these soft rollers and their comparison to rigid rollers are discussed later in Section III of the paper.

The membrane used to give the robot its toroidal shape was made out of thermoplastic polyurethane (TPU). We chose this material based on its commercial availability, its low cost, and the ability of this material to create airtight seals when heated (e.g., using an impulse or roller sealers) [14, 18]. Our robot uses air as the working fluid because of its ease of use and wide availability. However, other non-conductive fluids could also be used as working fluids, similar to water snake toys.

Chapter 2

Experimental Results

2.1 Comparison of Rigid and Soft Rollers

As mentioned above, we found a primary challenge of eversion locomotion on granular media to be grains getting in between the everting membrane and jamming the feeding mechanism. The rollers needed to be pre-tensioned to minimize slipping and maximize traction force while in use. We tuned this pre-tension using two set screws that pushed the motors towards each other. However, this also caused jamming issues as any grain particles trying to pass through the mechanism would get stuck. We hypothesized that a compliant structure would enable grains pass through the rollers without sacrificing traction force. To test this hypothesis, we designed feeding rollers with a silicone (Zhermack Elite Double 22) outer layer to provide a compliant structure to allow grains pass through when necessary. The soft rollers consisted of a core 3D printed from polylactic acid (PLA) and a molded silicone outer layer with a thickness of 5.8 mm, diameter of 34 mm, and length of 40 mm. The mold consisted of three parts which enabled an easy release (Fig. 2.1(a)). After the roller was cured, it was glued to the 3D printed core using super glue to prevent it from slipping. We used the same method of pre-tensioning for soft rollers as well. To validate the performance in terms of traction force compared to rigid rollers, we conducted the following experiment (see Fig. 2.1(b)): We secured the main body of the robot to a vice and connected the motors to a DC power supply. We passed two layers of the TPU membrane through the rollers and attached them to a force sensor (Mark-10 Force Gauge Model

M7-50). We set the force sensor to be stationary and applied electrical potential to the motors. We collected data using the force sensor while the motors were pulling the TPU sheets down and repeated the experiment five times for each case. We found that even without sand grains, the soft rollers provided a higher pulling force than rigid rollers (i.e., a maximum of 50 N as opposed to 15 N, see Fig. 2.1(c)). Soft rollers not only provided more force but also enabled grains to pass through freely by deforming when grains were passing through. Soft rollers enabled 27 g of 0.3 mm glass beads pass through in a minute. By comparison, the rigid rollers jammed when a single grain was introduced into the membrane.

2.2 Effect of Internal Pressure on Locomotion

Since the everted robot relied on internal pressure to maintain its shape and enable eversion, we experimentally investigated the effect of air pressure inside the membrane on the speed of the robot locomoting on sand. However, we did not have an easy way to directly measure the pressure inside of the robot due to the membrane. Thus, we conducted an indentation test using a mechanical testing apparatus (Mark-10 Force Gauge Model M7-50, Mark-10 Motorized Test Stand Model ESM750S). For this test, the mechanical tester pressed the force sensor into the membrane to a displacement of 6 mm, and measured the force as an indicator for pressure inside the membrane (Fig. 2.2(b)). Three different pressures were tested by letting out air between trials. Then, we put the robot on the surface of a layer of 0.3 mm glass beads to test its locomotion capabilities on a sand simulant. We recorded video of this locomotion from above (see Fig. 2.2(a); note that we added two lines to the membrane highlight the everting motion of the robot). We subsequently analyzed the recorded video using video analysis software (Tracker [19]) to collect position data (Fig. 2.2(c)).

We found out that the high pressure and medium pressure settings had average speeds of 3.38 cm/s and 3.39 cm/s, respectively, whereas the low setting had an average speed of 2.27 cm/s. The pressure inside the membrane in the low pressure trial wasn't high enough to lift the

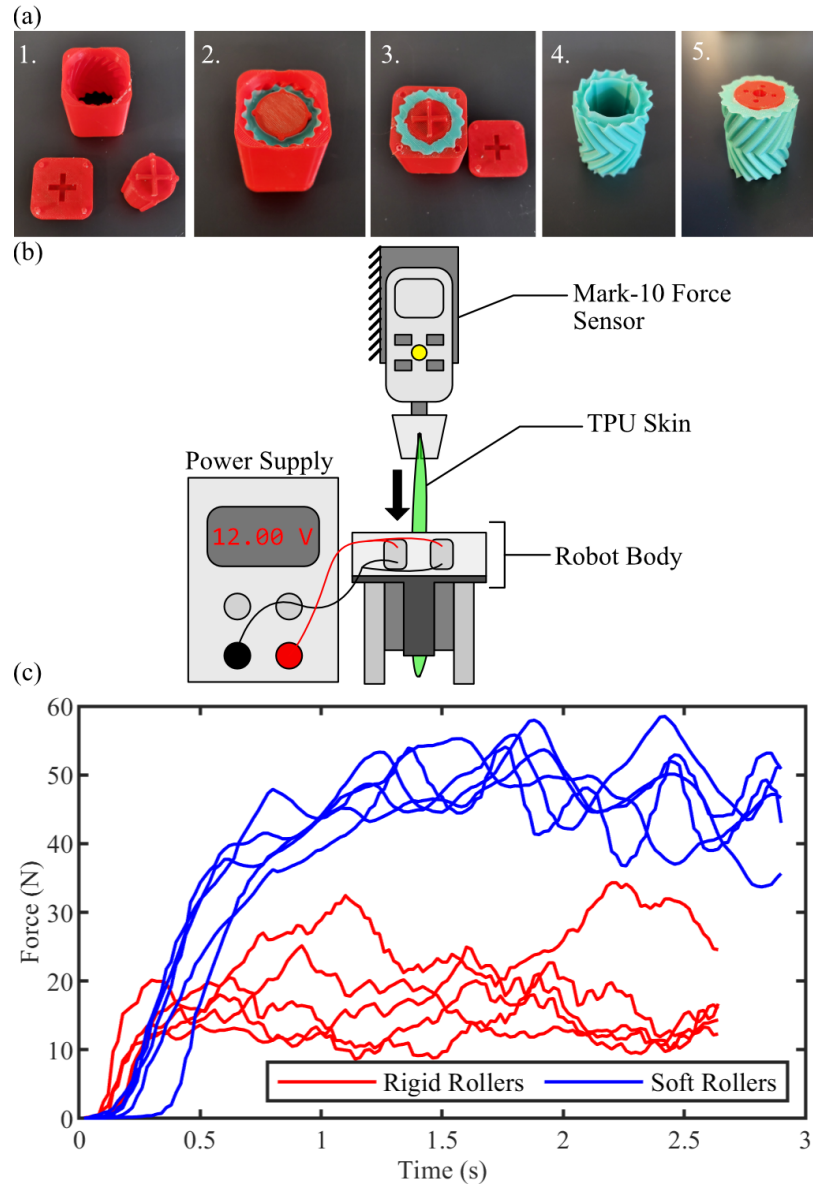


Figure 2.1. (a) Process for the fabrication of soft rollers used in the robot to avoid jamming due to sand grains. (b) Experimental setup using Mark-10 force sensor to compare soft and rigid rollers. (c) Plot of experimental results highlighting the difference in force for soft and rigid rollers.

robot body (i.e., 3D-printed rigid part of the robot) completely off of the ground, adding friction that resulted in a slower average speed. The high and medium pressure performed similarly indicating that there was a threshold pressure to pass for the robot to evert effectively.

2.3 Performance of the Robot in Digging

To evaluate the digging performance of our robot, we conducted an experiment in which the robot everted into a bucket filled with 0.3 mm glass beads (see Fig. 6a). We set up a camera in front of the bucket to record visual data (see Fig. 2.3(a)). We turned on the robot for 3 minutes, while recording a video. Later, we analyzed the videos using a tracker software (Tracker [19]) to gather. We turned on the robot for 3 minutes, while recording a video. Later, we analyzed the videos using a tracker software to gather position data. One limitation in this experiment was the need to stabilize the robot during the testing. This was a result of the inability of the soft membrane to support the mass of the components of the robot. To minimize this effect, we held the robot perpendicular to the granular surface during the experiment without exerting any downward force and without preventing it from everting. We present the results of the experiment in the form of a plot of vertical displacement versus time (see Fig. 2.3(c)) for three trials with their best fit line drawn. Using the three best fit lines, we found the average digging speed of the robot to be 3.92 mm/s with an efficiency of 12%. The low efficiency was due to the skin of the robot moving faster than the digging speed of the robot against the sand simulant, resulting in a lower speed compared to its locomotion speed on sand simulant. The slower speed of the robot in Trial 2 in red could be due to inaccuracies in the pressure inside the membrane of the robot as well as leakages. The noise in the data is due to the robot moving around in the horizontal axis while digging into granular media as well as moving in and out of the page, distorting 2D position data gathered using the camera. The results show the capability of our robot to dig itself in granular media.

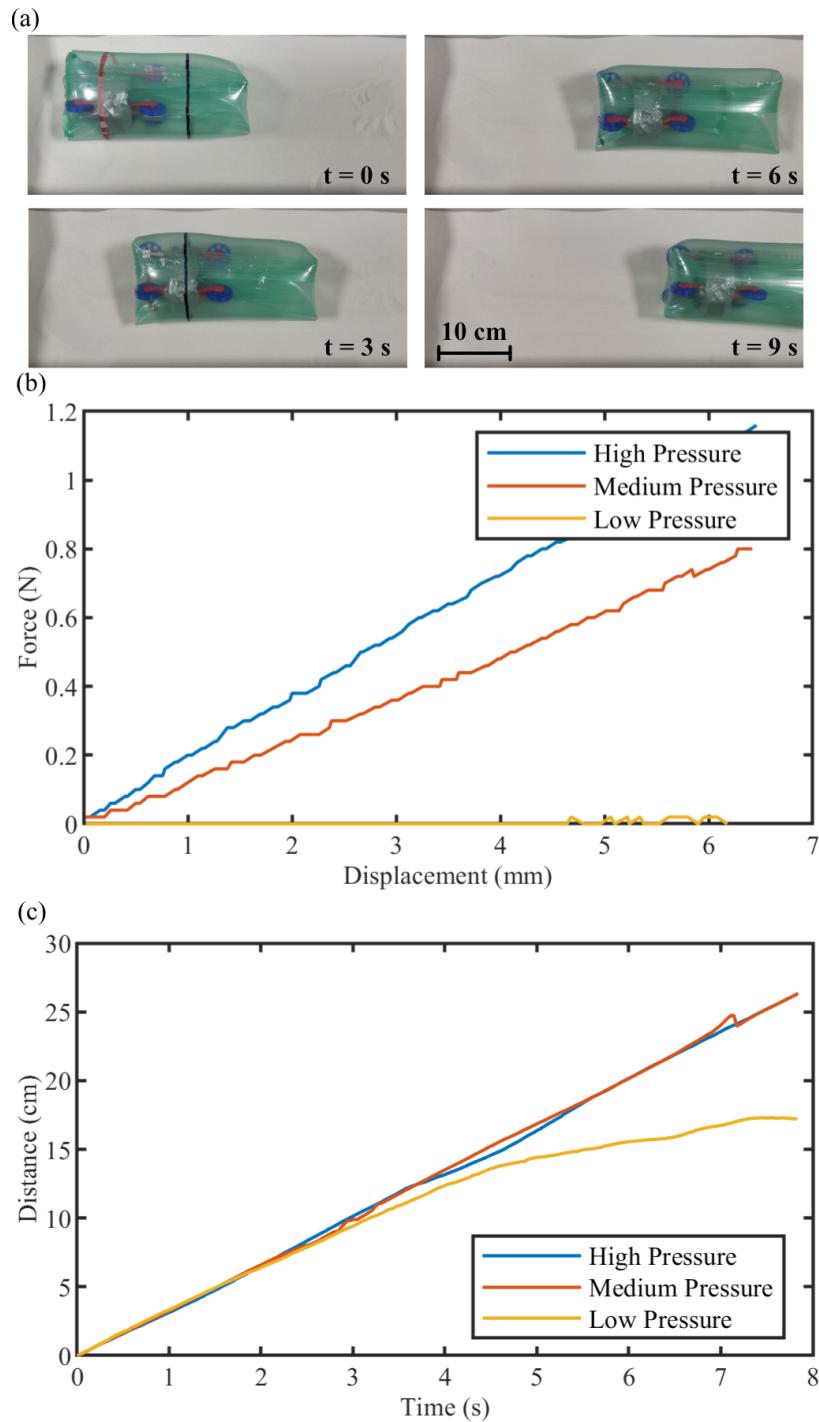


Figure 2.2. (a) Photos of the robot locomoting on sand from above at discrete time points (b) Plot of indentation experiment to determine the relative pressure inside the membrane for three different pressures (c) Plot of distance of the robot vs. time for three trials with different pressures. The high and medium pressures perform similarly whereas the low pressure was much slower

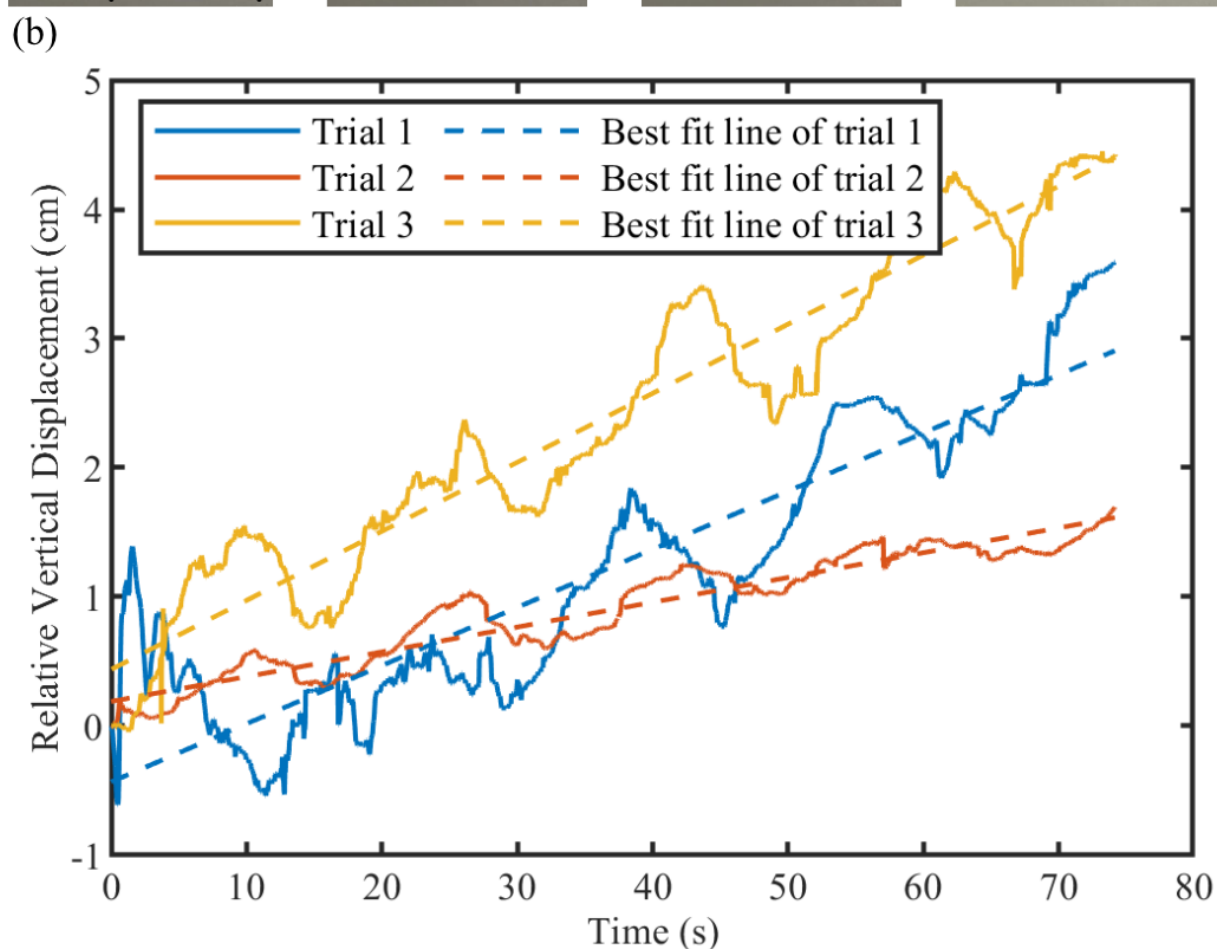
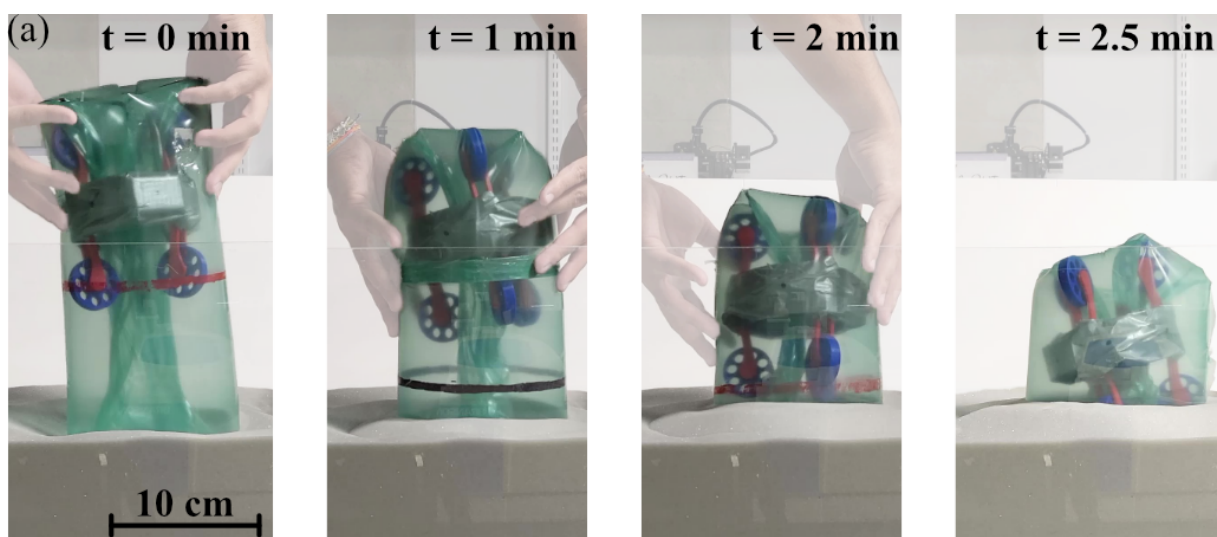


Figure 2.3. (a) Photos of the experiment at different discrete time intervals showing the robot's vertical displacement (b) Plot of vertical displacement vs time for multiple trials with raw and best fit lines shown

2.4 Performance of the Robot in Upward Burrowing

In addition to digging, the ability of burrowing upward is also important for robots in granular media. In order to test our robot's ability to burrow itself upward, we conducted a simple experiment in which the robot was buried in a bucket filled with 0.3 mm glass beads (see Fig.2.4). We set up a camera, recording video from the side to observe the robot as well as timing how long it takes to un-burrow itself. The experiment was repeated three times and the vertical position of the top part of the skin was tracked using a tracking software (Tracker [19]). A Primary challenge of burrowing upward was increased pressure on the robot by the surrounding granular media caused robot to lose internal pressure rapidly. This prevented the robot to continue everting and burrowing upward. To overcome this challenge, we used two layers of TPU skin heat pressed together to fabricate a thicker skin (0.06 mm). Thicker skin helped to keep the pressure inside for longer periods as well as reducing small holes on the skin around heat sealed parts. We present the results in the form of a plot of absolute vertical displacement versus time (see Fig. 2.5) for three trials with their best fit line drawn. The average upward burrowing speed of the robot is found to be 1.76 cm/s over three trials. The efficiency of the robot was 54% compared to locomtion on sand. This was due to skin slipping against the sand. The decrease in the vertical displacement towards the end of the experiment was due to robot leaning to one side as it got out of the granular media, distorting vertical displacement data gathered using the camera. The results show the capability of our robot to dig itself out in granular media. In comparison, it took 30.10 N on average between three trials to pull the robot out of the sand simulant when it was buried at one body length depth. We also tested our robot's anchoring capability. By comparing the peak pull-out force required (see Fig.2.6 for the experimental setup), we found that it took 75.07 N on average between three trials to pull out the robot when it was deflated under sand simulant, an increase of 250%. On the other hand, our robot was able to burrow upwards without any external force, applying force to its environment. The results show the capability of our robot to dig itself out in granular media.

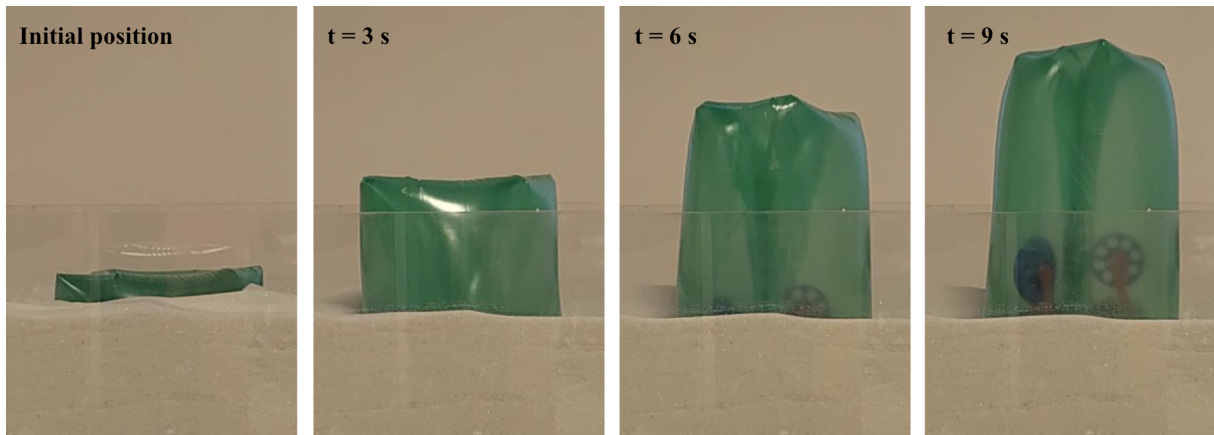


Figure 2.4. Photos of the third trial at different discrete time intervals showing robot burrowing upward over time. Timestamps represents the time after the robot was turned on.

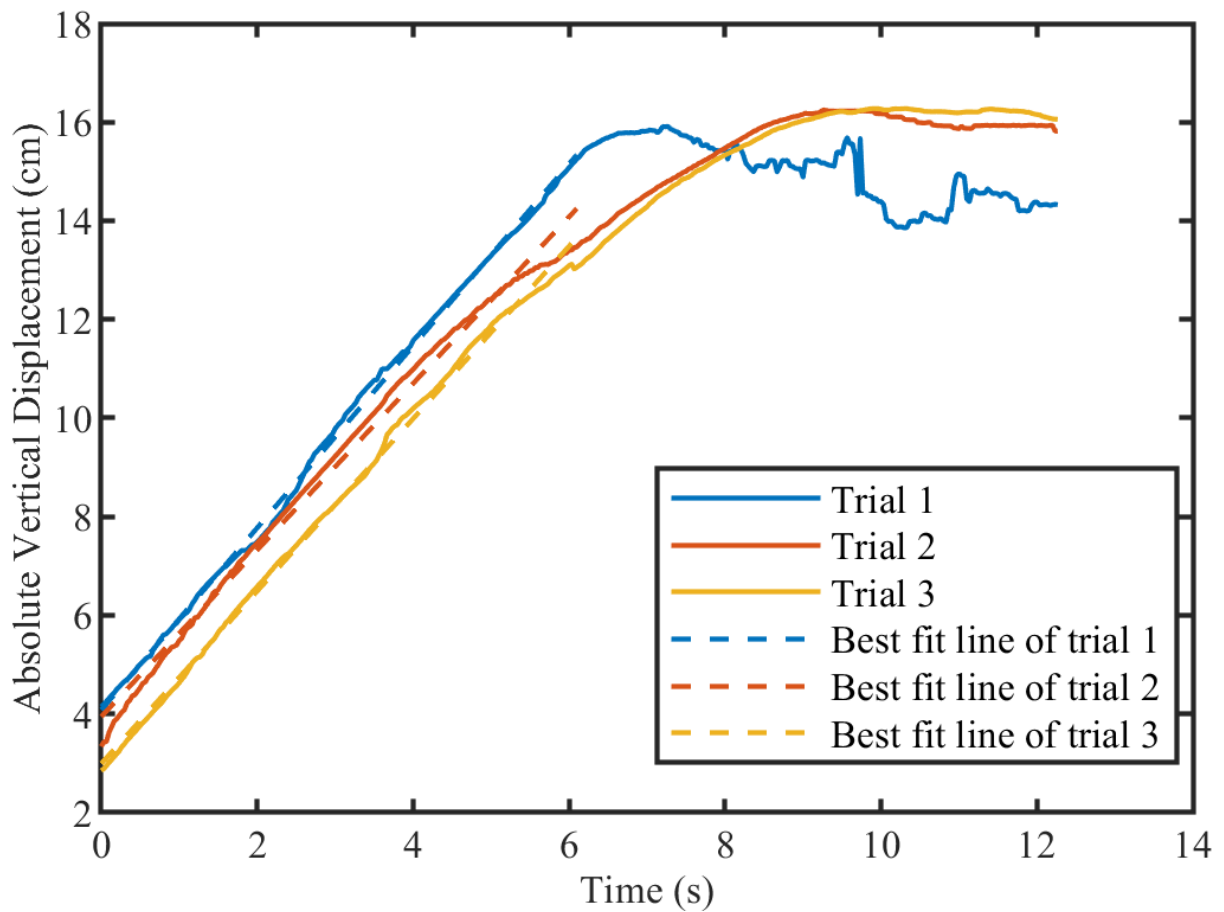


Figure 2.5. Plot of absolute vertical displacement versus time for multiple trials with best fit lines shown dashed lines

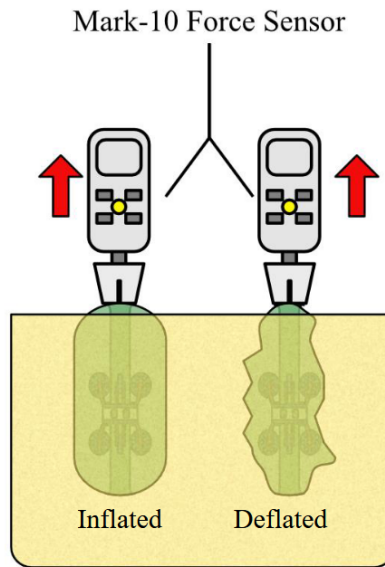


Figure 2.6. Experimental setup showing the difference between the two cases of inflated and deflated robot when comparing the peak pull-out force using the Mark-10 Force sensor.

2.5 Locomotion on Water

In addition to exploration on and within sand, we tested the ability of our robot to achieve amphibious exploration on the surface of water. We turned on the robot and put it in an aquarium filled with water and containing fake aquatic plants. Since the main body of the robot that contained all the electronics was already encapsulated by the skin, our robot was waterproof by design. With the help of a camera and the tracker software used for the previous experiments [19], we recorded the initial and final position of the main body of the robot. Our robot was able to locomote on water with an average speed of 2.9 cm/s with an efficiency of 87% (compared to its locomotion speed on sand) since the skin of the robot moved faster than the locomotion speed of the robot against the surface of water, which reduced its efficiency (see Fig.2.7). The robot was also able to locomote above the plastic seaweed that was placed in the tank, highlighting its ability to achieve amphibious locomotion.

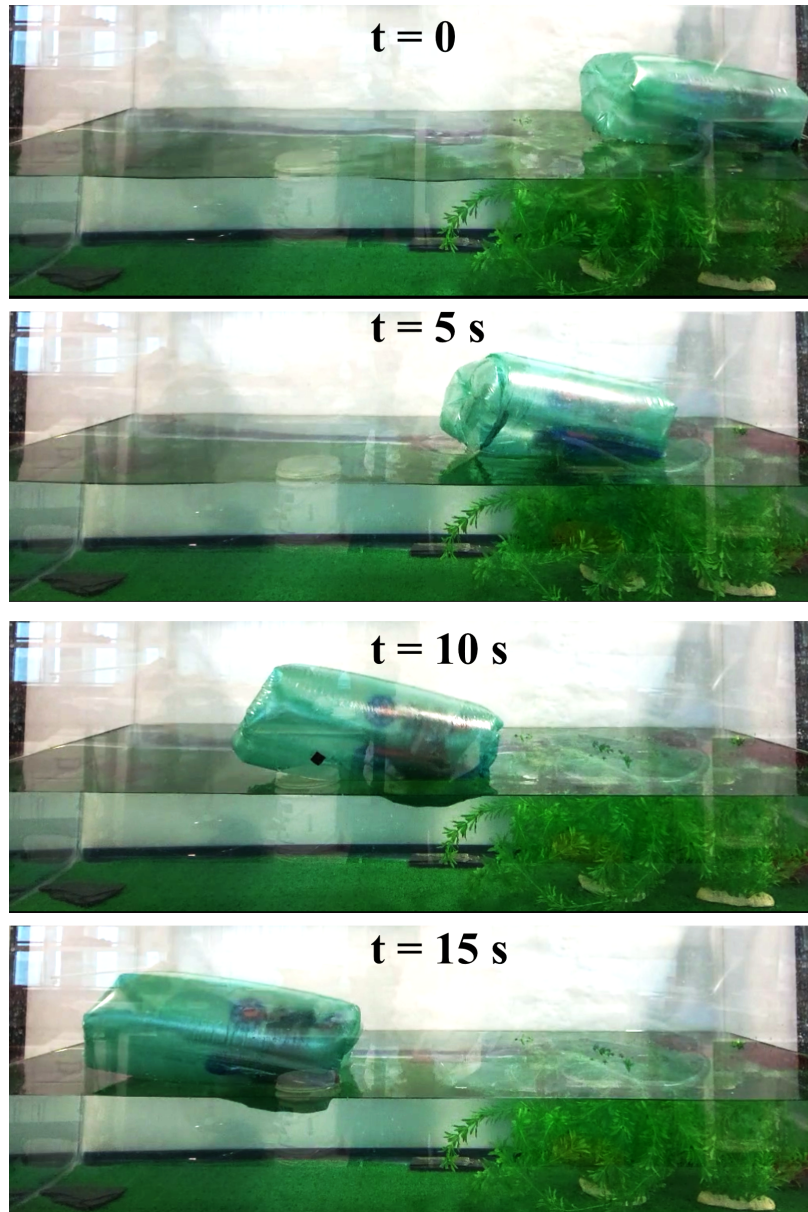


Figure 2.7. Photos of the experiment at different discrete time intervals showing the robot's locomotion on water

Conclusion

To conclude, we presented a soft everting robot capable of locomoting on sand as well as digging in sand in an untethered fashion. We highlighted the important design considerations that improved the performance of the robot in granular media. Our experimental results show that the toroidal shape allowed us to design an untethered eversion robot with a similar reduction of drag force seen in tethered eversion vine robots. In addition, experimental results confirmed that the use of soft rollers provides a better traction to prevent slipping as well as providing a compliant structure to let foreign objects such as grains to pass through the rollers freely. We showed that our robot was able to dig itself both into and out of granular media. The successful downward and upward burrowing experiments validated our hypothesis that continuous skin eversion can enable digging.

Applications of this work range from pipe inspection to sensor placement in granular media for environmental monitoring. Future work could investigate different skin features and different working fluids to increase digging and locomotion performance in granular media. In addition, the effects of different actuation cycles such as periodic actuation instead of constant actuation on the digging performance could be studied. One could also study the optimization of the design's size and shape to increase its performance in granular media.

I would like to acknowledge Professor Michael Tolley and Professor Nicholas Gravish for coauthoring this thesis in full, a major portion of which has been published in the proceedings of the IEEE International Conference on Soft Robotics and on IEEE Xplore. The thesis author was the primary investigator and author of this material.

Bibliography

- [1] S. W. Squyres, R. E. Arvidson, D. Bollen, J. F. Bell III, J. Brückner, N. A. Cabrol, W. M. Calvin, M. H. Carr, P. R. Christensen, B. C. Clark, L. Crumpler, D. J. Des Marais, C. d’Uston, T. Economou, J. Farmer, W. H. Farrand, W. Folkner, R. Gellert, T. D. Glotch, M. Golombek, S. Gorevan, J. A. Grant, R. Greeley, J. Grotzinger, K. E. Herkenhoff, S. Hviid, J. R. Johnson, G. Klingelhöfer, A. H. Knoll, G. Landis, M. Lemmon, R. Li, M. B. Madsen, M. C. Malin, S. M. McLennan, H. Y. McSween, D. W. Ming, J. Moersch, R. V. Morris, T. Parker, J. W. Rice Jr., L. Richter, R. Rieder, C. Schröder, M. Sims, M. Smith, P. Smith, L. A. Soderblom, R. Sullivan, N. J. Tosca, H. Wänke, T. Wdowiak, M. Wolff, and A. Yen, “Overview of the opportunity mars exploration rover mission to meridiani planum: Eagle crater to purgatory ripple,” *Journal of Geophysical Research: Planets*, vol. 111, no. E12, 2006.
- [2] G. Bribiesca-Contreras, T. G. Dahlgren, D. J. Amon, S. Cairns, R. Drennan, J. M. Durden, M. P. Eléaume, A. M. Hosie, A. Kremenetskaia, K. McQuaid, T. D. O’Hara, M. Rabone, E. Simon-Lledó, C. R. Smith, L. Watling, H. Wiklund, and A. G. Glover, “benthic megafauna of the western clarion-clipperton zone, pacific ocean,” *ZooKeys*, vol. 1113, pp. 1–110, 2022.
- [3] R. D. Maladen, Y. Ding, P. B. Umbanhowar, A. Kamor, and D. I. Goldman, “Mechanical models of sandfish locomotion reveal principles of high performance subsurface sand-swimming,” *Journal of The Royal Society Interface*, vol. 8, no. 62, pp. 1332–1345, 2011.
- [4] G. Girmscheid and C. Schexnayder, “Tunnel boring machines,” 2009.
- [5] D. Ortiz, N. Gravish, and M. T. Tolley, “Soft robot actuation strategies for locomotion in granular substrates,” *IEEE Robotics and Automation Letters*, vol. 4, no. 3, pp. 2630–2636, 2019.
- [6] Y. Ozkan Aydin, B. Liu, A. Ferrero, M. Seidel, F. Hammond, and D. Goldman, “Lateral bending and buckling aids biological and robotic earthworm anchoring and locomotion,” *Bioinspiration Biomimetics*, vol. 17, 09 2021.
- [7] A. Sadeghi, A. Mondini, and B. Mazzolai, “Toward self-growing soft robots inspired by plant roots and based on additive manufacturing technologies,” *Soft Robotics*, vol. 4, no. 3, pp. 211–223, 2017. PMID: 29062628.

- [8] J. J. Tao, S. Huang, and Y. Tang, “Sbor: a minimalistic soft self-burrowing-out robot inspired by razor clams,” *Bioinspiration & Biomimetics*, vol. 15, 2020.
- [9] J. Luong, P. Glick, A. Ong, M. S. deVries, S. Sandin, E. W. Hawkes, and M. T. Tolley, “Eversion and retraction of a soft robot towards the exploration of coral reefs,” in *2019 2nd IEEE International Conference on Soft Robotics (RoboSoft)*, pp. 801–807, 2019.
- [10] N. D. Naclerio, A. Karsai, M. Murray-Cooper, Y. Ozkan-Aydin, E. Aydin, D. I. Goldman, and E. W. Hawkes, “Controlling subterranean forces enables a fast, steerable, burrowing soft robot,” *Science Robotics*, vol. 6, no. 55, p. eabe2922, 2021.
- [11] V. Orekhov, M. Yim, and D. Hong, “Mechanics of a Fluid Filled Everting Toroidal Robot for Propulsion and Going Through a Hole,” vol. Volume 2: 34th Annual Mechanisms and Robotics Conference, Parts A and B of *International Design Engineering Technical Conferences and Computers and Information in Engineering Conference*, pp. 1205–1212, 08 2010.
- [12] D. W. Hong, M. Ingram, and D. Lahr, “Whole Skin Locomotion Inspired by Amoeboid Motility Mechanisms,” *Journal of Mechanisms and Robotics*, vol. 1, 09 2008. 011015.
- [13] H. Leon-Rodriguez, V. H. Le, S. Y. Ko, J.-O. Park, and S. Park, “Ferrofluid soft-robot bio-inspired by amoeba locomotion,” in *2015 15th International Conference on Control, Automation and Systems (ICCAS)*, pp. 1833–1838, 2015.
- [14] N. G. B. Perez and M. M. Coad, “Self-propelled soft everting toroidal robot for navigation and climbing in confined spaces,” in *2022 IEEE/RSJ International Conference on Intelligent Robots and Systems (IROS)*, pp. 5409–5415, 2022.
- [15] ISO, “Geotechnical investigation and testing — identification and classification of soil — part 1: Identification and description.” <https://www.iso.org/standard/66345.html>, 2017. Accessed: 2023-04-30.
- [16] M. M. Coad, R. P. Thomasson, L. H. Blumenschein, N. S. Usevitch, E. W. Hawkes, and A. M. Okamura, “Retraction of soft growing robots without buckling,” *IEEE Robotics and Automation Letters*, vol. 5, no. 2, pp. 2115–2122, 2020.
- [17] S.-G. Jeong, M. Coad, L. Blumenschein, M. Luo, U. Mehmood, J. Kim, A. Okamura, and J.-H. Ryu, “A tip mount for transporting sensors and tools using soft growing robots,” pp. 8781–8788, 10 2020.
- [18] P. Glick, I. Adibnazari, D. Drotman, D. Ruffatto, and M. Tolley, “Branching vine robots for unmapped environments,” *Frontiers in Robotics and AI*, vol. 9, p. 838913, 03 2022.
- [19] R. E. Arvidson, R. C. Anderson, P. Bartlett, J. F. Bell, D. Blaney, P. R. Christensen, P. Chu, L. Crumpler, K. Davis, B. L. Ehlmann, R. Fergason, M. P. Golombek, S. Gorevan, J. A. Grant, R. Greeley, E. A. Guinness, A. F. C. Haldemann, K. Herkenhoff, J. Johnson, G. Landis, R. Li, R. Lindemann, H. McSween, D. W. Ming, T. Myrick, L. Richter, F. P.

Seelos, S. W. Squyres, R. J. Sullivan, A. Wang, and J. Wilson, "Localization and physical properties experiments conducted by spirit at gusev crater," *Science*, vol. 305, no. 5685, pp. 821–824, 2004.